The WiggleZ Dark Energy Survey: measuring the cosmic expansion history using the Alcock–Paczynski test and distant supernovae

Chris Blake,[1]* Karl Glazebrook,[1] Tamara M. Davis,[2,3] Sarah Brough,[4] Matthew Colless,[4] Carlos Contreras,[1] Warrick Couch,[1] Scott Croom,[5] Michael J. Drinkwater,[2] Karl Forster,[6] David Gilbank,[7] Mike Gladders,[8] Ben Jelliffe,[5] Russell J. Jurek,[9] I-hui Li,[1] Barry Madore,[10] D. Christopher Martin,[6] Kevin Pimbblet,[11] Gregory B. Poole,[1] Michael Pracy,[1,12] Rob Sharp,[2,12] Emily Wisnioski,[1] David Woods,[13] Ted K. Wyder[6] and H. K. C. Yee[14]

[1]*Centre for Astrophysics and Supercomputing, Swinburne University of Technology, PO Box 218, Hawthorn, VIC 3122, Australia*
[2]*School of Mathematics and Physics, University of Queensland, Brisbane, QLD 4072, Australia*
[3]*Dark Cosmology Centre, Niels Bohr Institute, University of Copenhagen, Juliane Maries Vej 30, DK-2100 Copenhagen Ø, Denmark*
[4]*Australian Astronomical Observatory, PO Box 296, Epping, NSW 1710, Australia*
[5]*Sydney Institute for Astronomy, School of Physics, University of Sydney, Sydney, NSW 2006, Australia*
[6]*California Institute of Technology, MC 278-17, 1200 East California Boulevard, Pasadena, CA 91125, USA*
[7]*Astrophysics and Gravitation Group, Department of Physics and Astronomy, University of Waterloo, Waterloo, ON N2L 3G1, Canada*
[8]*Department of Astronomy and Astrophysics, University of Chicago, 5640 South Ellis Avenue, Chicago, IL 60637, USA*
[9]*Australia Telescope National Facility, CSIRO, Epping, NSW 1710, Australia*
[10]*Observatories of the Carnegie Institute of Washington, 813 Santa Barbara St., Pasadena, CA 91101, USA*
[11]*School of Physics, Monash University, Clayton, VIC 3800, Australia*
[12]*Research School of Astronomy and Astrophysics, Australian National University, Weston Creek, ACT 2611, Australia*
[13]*Department of Physics and Astronomy, University of British Columbia, 6224 Agricultural Road, Vancouver, BC V6T 1Z1, Canada*
[14]*Department of Astronomy and Astrophysics, University of Toronto, 50 St George Street, Toronto, ON M5S 3H4, Canada*

ABSTRACT

Astronomical observations suggest that today's Universe is dominated by a dark energy of unknown physical origin. One of the most notable results obtained from many models is that dark energy should cause the expansion of the Universe to accelerate: but the expansion rate as a function of time has proved very difficult to measure directly. We present a new determination of the cosmic expansion history by combining distant supernovae observations with a geometrical analysis of large-scale galaxy clustering within the WiggleZ Dark Energy Survey, using the Alcock–Paczynski test to measure the distortion of standard spheres. Our result constitutes a robust and non-parametric measurement of the Hubble expansion rate as a function of time, which we measure with 10–15 per cent precision in four bins within the redshift range $0.1 < z < 0.9$. We demonstrate, in a manner insensitive to the assumed cosmological model, that the cosmic expansion is accelerating. Furthermore, we find that this expansion history is consistent with a cosmological-constant dark energy.

Key words: surveys – dark energy – distance scale.

1 INTRODUCTION

Observations by astronomers over the past 15 years suggest that the Universe is dominated by an unexpected component known as 'dark energy', yet we still have no physical understanding of its existence or magnitude. Determining the nature of dark energy is one of the most important challenges for contemporary cosmology because its presence implies that our understanding of the physics of the Universe is incomplete. Possible explanations are that the theory of General Relativity must be modified on cosmological scales to explain an effective repulsive gravitational force, the Universe is filled with a diffuse material that acts with an effective negative pressure, or our interpretation of cosmological observations must be changed to reflect inhomogeneities.

*E-mail: cblake@astro.swin.edu.au

One of the most important consequences of the first two scenarios is that the Universe underwent a transition from decelerating to accelerating expansion within the last few billion years. In this paper we use new observations and methods to map this expansion history in a model-insensitive, non-parametric and robust manner.

In the standard cosmological analyses, involving data sets such as distant supernovae (Riess et al. 1998; Perlmutter et al. 1999; Amanullah et al. 2010; Conley et al. 2011), galaxy surveys (Giannantonio et al. 2008; Percival et al. 2010; Blake et al. 2011a) and the cosmic microwave background radiation (Komatsu et al. 2011), the expansion rate of the Universe at different look-back times is not measured directly. Accelerating expansion is a *model-dependent implication of fitting cosmological data with parametric models* in which prior assumptions are made about the physical components of the Universe and their evolution with redshift. However, the unknown physical nature of dark energy implies that we cannot yet be certain that any particular parametric model is correct.

For example, measurements of distant supernovae provide some of the strongest evidence for the existence of dark energy. The observed quantities are the apparent magnitudes of the supernovae, which yield a relative luminosity distance as a function of redshift, i.e. $D_L(z) H_0/c$, where $D_L(z)$ is the luminosity distance, H_0 is the local value of the Hubble expansion rate and c is the speed of light. These supernovae distances are well fitted by a model in which the physical contents of the Universe are divided into pressureless matter with a current fractional energy density Ω_m, which dilutes with redshift as $(1 + z)^3$, and a 'cosmological constant' Ω_Λ whose energy density does not change with redshift. The best-fitting parameters assuming this model are $\Omega_m \approx 0.27$ and $\Omega_\Lambda \approx 0.73$, implying a transition from decelerating to accelerating expansion at $z \approx 0.6$ (e.g. Conley et al. 2011).

However, this conclusion is dependent on the assumed parametrized model. The acceleration of the expansion rate is not directly observed. When the supernovae data are subject to model-independent *non-parametric analysis*, the evidence for accelerating expansion is much weaker (Wang & Tegmark 2005; Shapiro & Turner 2006; Shafieloo 2007; Sollerman et al. 2009; Shafieloo & Clarkson 2010). This is primarily because the acceleration rate is obtained as the second derivative of the noisy observed luminosity distances. Moreover, obtaining the cosmic expansion rate from a luminosity distance requires an additional assumption about spatial curvature. Although recent cosmological data are consistent with a spatially flat Universe (Percival et al. 2010; Komatsu et al. 2011), this conclusion is again reached within the assumption of a parametrized model (unless we invoke a strong prior from inflationary cosmological models).

The expansion history of the Universe as a function of redshift z is described by the evolution of the Hubble parameter $H(z) \equiv (1 + z)\, da/dt$, where $a(t)$ is the cosmic scalefactor at time t. In this paper we present a new determination of the function $H(z)$ using a two-step approach. First we apply an Alcock–Paczynski measurement (Alcock & Paczynski 1979) to the large-scale clustering of galaxies in the WiggleZ Dark Energy Survey (Drinkwater et al. 2010), thereby measuring the distortion parameter $F(z) \equiv (1 + z)D_A(z)H(z)/c$, where $D_A(z)$ is the physical angular-diameter distance. Secondly, we combine this measurement with the supernovae luminosity distances $D_L(z) H_0/c$, using the equivalence of distance measurements $D_L(z) = D_A(z)(1 + z)^2$, to infer the value of $H(z)/H_0$. The result is an accurate non-parametric reconstruction of the cosmic expansion history, which is independent of the assumed cosmological model (including spatial curvature). We present our

results in the form of both individual measurements of $H(z)/H_0$ in four redshift bins within the redshift range $0.1 < z < 0.9$, and a non-parametric reconstruction of a continuous cosmic expansion history using a modified version of the iterative methods introduced by Shafieloo et al. (2006).

Other methods for determining the Hubble expansion rate have been previously attempted. First, $H(z)$ may be inferred from the relative ages of passively evolving galaxies (Stern et al. 2010). This is a promising technique although subject to many assumptions about the stellar populations and formation epochs of these galaxies. Secondly, the imprint of baryon acoustic oscillations in galaxy clustering has been applied as a standard ruler along the line of sight (Gaztanaga, Cabre & Hui 2009). However, the current availability of large-scale galaxy survey data restricts this latter technique to low redshifts, $z = 0.35$, and it is debatable whether the signal-to-noise ratio of current measurements is in fact sufficient to ensure a robust measurement (Kazin et al. 2009). Finally, the physical presence of dark energy has been inferred from the late-time integrated Sachs–Wolfe effect which correlates low-redshift galaxy overdensities with cosmic microwave background (CMB) anisotropies (Giannantonio et al. 2008). However, this last technique does not allow recovery of the detailed expansion history and the achievable statistical significance is limited.

The Alcock–Paczynski test (Alcock & Paczynski 1979) is a geometric probe of the cosmological model based on the comparison of the observed tangential and radial dimensions of objects which are assumed to be isotropic for the correct choice of model. It can be applied to the two-point statistics of galaxy clustering if redshift-space distortions, the principal additional source of anisotropy, can be successfully modelled (Ballinger, Peacock & Heavens 1996; Matsubara & Suto 1996; Matsubara 2000; Seo & Eisenstein 2003; Simpson & Peacock 2010). This method has been previously utilized with data from the 2-degree Field Quasar Survey (Outram et al. 2004), but the WiggleZ survey offers a superior measurement owing to the reduced importance of shot noise. Chuang & Wang (2011) recently performed fits to the tangential and radial clustering of luminous red galaxies within the Sloan Digital Sky Survey (SDSS) at redshift $z = 0.35$, utilizing Alcock–Paczynski information. Indeed, a general analysis of the tangential/radial galaxy clustering pattern in the presence of baryon acoustic oscillations demonstrates how the information may be divided into an overall scale distortion, quantified by a distance parameter $D_V \propto (D_A^2/H)^{1/3}$, and a warping, quantified by the Alcock–Paczynski distortion factor $D_A H$, enabling the disentangling of D_A and H (Padmanabhan & White 2008; Kazin, Sanchez & Blanton 2011; Taruya, Saito & Nishimichi 2011). Such approaches are just becoming possible with the current generation of large-scale galaxy surveys, and will be very powerful when applied to future data sets such as the Baryon Oscillation Spectroscopic Survey (BOSS, Eisenstein et al. 2011). Another recent application of the Alcock–Paczynski test was presented by Marinoni & Buzzi (2010), who presented a study of the distribution of close galaxy pairs.

The WiggleZ Dark Energy Survey (Drinkwater et al. 2010) at the Australian Astronomical Observatory has recently provided a new large-scale galaxy redshift survey data set, allowing low-redshift cosmological measurements in the SDSS to be extended to higher redshifts up to $z = 0.9$. In particular, the survey has yielded a measurement of the baryon acoustic peak in the clustering pattern at $z = 0.6$ (Blake et al. 2011b). In addition, Blake et al. (2011a) mapped the growth of cosmic structure in this data set across the redshift range $0.1 < z < 0.9$ for a fixed background cosmological model. The new study presented in this paper constitutes a generalization

of that analysis incorporating Alcock–Paczynski distortions arising in varying cosmological models.

Our paper is structured as follows. In Section 2 we introduce the WiggleZ survey data set and power spectrum measurements. In Section 3 we describe our implementation of the Alcock–Paczynski test and our model for marginalizing over redshift-space distortions. In Section 4 we combine these Alcock–Paczynski measurements with supernovae data to deduce the expansion history $H(z)$. In Section 5 we present a non-parametric reconstruction of the continuous cosmic expansion history, and we summarize our findings in Section 6.

2 WIGGLEZ SURVEY POWER SPECTRA

2.1 The WiggleZ Dark Energy Survey

The WiggleZ Dark Energy Survey (Drinkwater et al. 2010) with the 3.9-m Anglo-Australian Telescope has provided the next step in large-scale spectroscopic galaxy redshift surveys, mapping a cosmic volume ~ 1 Gpc^3 over the redshift range $0 < z < 1$. By covering a total of about 800 deg^2 of sky, the WiggleZ survey has mapped about 100 times more effective cosmic volume in the $z > 0.5$ Universe than previous galaxy redshift surveys. Target galaxies were chosen by a joint selection in UV and optical wavebands, using observations by the *Galaxy Evolution Explorer* satellite (*GALEX*; Martin et al. 2005) matched with ground-based optical imaging from the Sloan Digital Sky Survey (York et al. 2000) in the Northern Galactic Cap, and from the Red-sequence Cluster Survey 2 (RCS2) (Gilbank et al. 2011) in the Southern Galactic Cap. A series of magnitude and colour cuts (Drinkwater et al. 2010) was used to preferentially select high-redshift star-forming galaxies with bright emission lines, which were then observed using the AAOmega multi-object spectrograph (Sharp et al. 2006) in 1-h exposures. In this study we analysed a galaxy sample drawn from our final set of observations, after cuts to maximize the contiguity of each survey region. The sample includes a total of 162 323 galaxy redshifts, which we divided into four different redshift slices of width $\Delta z = 0.2$ between $z = 0.1$ and 0.9. The numbers of galaxies analysed in the respective redshift slices were $N = (22\,072, 42\,160, 63\,737, 34\,354)$.

2.2 Power spectrum measurements

Our analysis is based on measurements of the power spectrum amplitude of WiggleZ galaxies as a function of the angle to the line of sight θ, which we parametrize by the variable $\mu = \cos\theta$. By comparing the amplitude of power spectrum modes as a function of μ we can apply an Alcock–Paczynski measurement as proposed by Ballinger et al. (1996) and Matsubara & Suto (1996) and described in Section 3. We measured galaxy power spectra in six independent survey regions, dividing each region into four redshift slices. At a given redshift we fitted models to the measurements in each of the different survey regions, convolving with the respective survey window function.

In order to measure the power spectrum and calculate this convolution, we need to define the selection function of the survey which describes the mean galaxy density as a function of position. The angular and redshift dependences of the selection function for each WiggleZ region were determined using the methods described by Blake et al. (2010). This process models several effects including the variation in the *GALEX* target density with dust and exposure time, the incompleteness of the current redshift catalogue, the variation of that incompleteness imprinted across each 2-degree field by constraints on the positioning of fibres and throughput variations with

fibre position, and the dependence of the galaxy redshift distribution on optical magnitude. The galaxy power spectrum was then measured using the optimal-weighting scheme proposed by Feldman, Kaiser & Peacock (1994). Our fiducial cosmological model which we use to convert redshifts and angular coordinates to distances is a flat ΛCDM model with matter density $\Omega_m = 0.27$.

Because the WiggleZ survey consists of a series of independent narrow-angle cones (of width $\approx 10°$ on the sky) a 'flat-sky' approximation may be used in which the coordinate x-axis is aligned with the line of sight at the centre of each region; the wavevector components (k, μ) are then deduced from the three-dimensional Fourier vector $\boldsymbol{k} = (k_x, k_y, k_z)$ as $k = \sqrt{k_x^2 + k_y^2 + k_z^2}$ and $\mu = |k_x|/k$. The observed power spectra were corrected for the small effect of redshift blunders (Blake et al. 2010). The covariance matrix of the power spectrum measurement was deduced using the methodology of Feldman et al. (1994), and the convolution matrices were determined from the window function as described in section 2.2 of Blake et al. (2011a). Fig. 1 displays the 2D power spectrum amplitudes as a function of (k, μ), stacked over the survey regions at each redshift.

The effective redshifts of the power spectrum measurements in each slice were $z = (0.22, 0.41, 0.6, 0.78)$, determined by weighting each pixel in the selection function by its contribution to the power spectrum error (Blake et al. 2010):

$$z_{\text{eff}} = \sum_{\boldsymbol{x}} z \left(\frac{n_g(\boldsymbol{x}) P_g}{1 + n_g(\boldsymbol{x}) P_g} \right)^2 , \tag{1}$$

where $n_g(\boldsymbol{x})$ is the galaxy number density in each grid cell $\boldsymbol{x}$ and P_g is the characteristic galaxy power spectrum amplitude, which we evaluated at a scale $k = 0.1\,h\,\text{Mpc}^{-1}$. We note that our results are not sensitive to the precise value of the effective redshift: the measured quantity is the scale distortion parameter $F(z_{\text{eff}}) \equiv (1 + z_{\text{eff}}) D_A(z_{\text{eff}}) H(z_{\text{eff}})$ *relative to its value in the fiducial cosmological model*, rather than the quantity $F(z_{\text{eff}})$ itself. In other words, if the effective redshift was in error by Δz_{eff}, then the systematic error in $F(z_{\text{eff}} + \Delta z_{\text{eff}})/F_{\text{fid}}(z_{\text{eff}} + \Delta z_{\text{eff}})$ can be negligible even when the difference between $F(z_{\text{eff}})$ and $F(z_{\text{eff}} + \Delta z_{\text{eff}})$ is not.

3 ALCOCK–PACZYNSKI MEASUREMENT

3.1 The Alcock–Paczynski effect

An Alcock–Paczynski measurement (Alcock & Paczynski 1979) is a method for constraining the cosmological model by comparing the observed tangential and radial dimensions of objects which are assumed to be isotropic, i.e. possess equal comoving tangential and radial sizes L_0. The observed tangential dimension is the angular projection $\Delta\theta = L_0/[(1 + z) D_A(z)]$. The observed radial dimension is the redshift projection $\Delta z = L_0 H(z)/c$. The intrinsic size L_0 does not need to be known in order to recover the observable $\Delta z/\Delta\theta = (1 + z) D_A(z) H(z)/c$, which is independent of any assumption about spatial curvature. It is not necessary that an Alcock–Paczynski measurement be applied to cosmological 'objects' but this test is equally valid for an isotropic process such as the two-point statistics of galaxy clustering (Ballinger et al. 1996; Matsubara & Suto 1996).

The relative tangential/radial distortion depends on the value of $F(z) = (1 + z) D_A(z) H(z)/c$ relative to the fiducial model (which we take as a flat ΛCDM cosmology with $\Omega_m = 0.27$, although the results do not depend significantly on this choice). We applied the
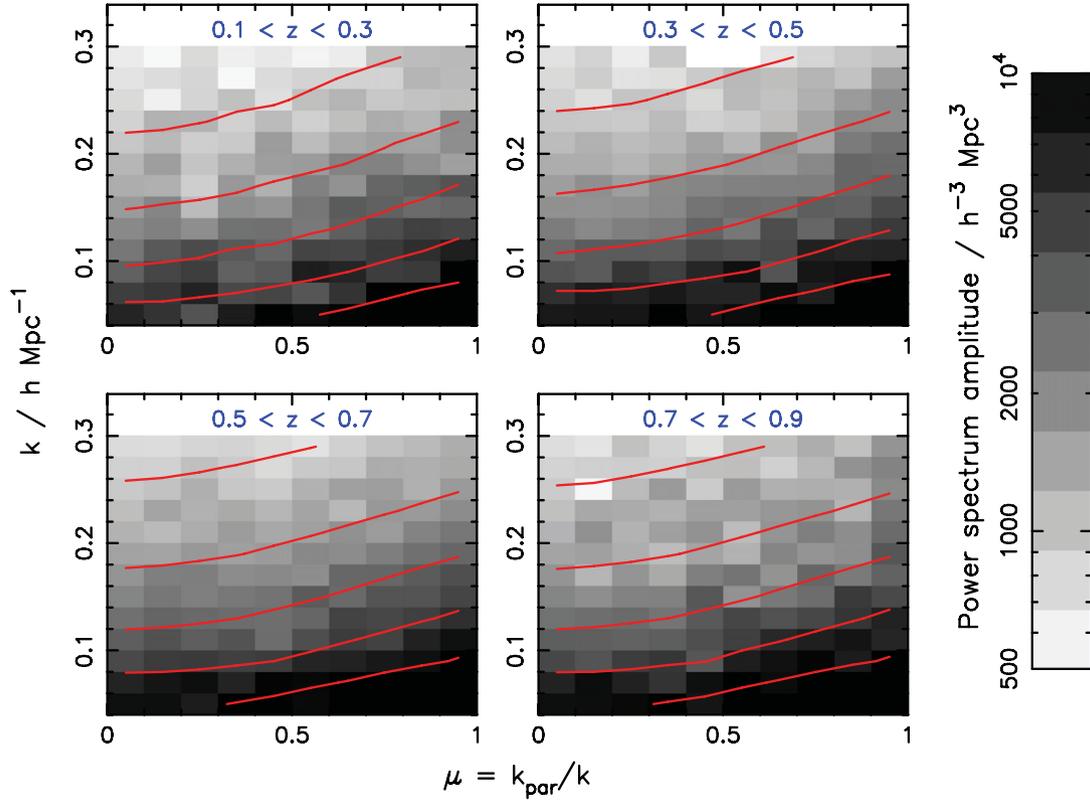
Figure 1. The galaxy power spectrum amplitude as a function of amplitude and angle of Fourier wavevector (k, μ), determined by stacking observations in different WiggleZ survey regions in four redshift slices. The contours correspond to the best-fitting non-linear redshift-space distortion model. We note that because of the differing degrees of convolution in each region due to the window function, a 'de-convolution' method was used to produce this plot. Before stacking, the data points were corrected by the ratio of the unconvolved and convolved two-dimensional power spectra corresponding to the best-fitting model, for the purposes of this visualization. In the absence of redshift-space distortions, the model contours would be horizontal lines if the fiducial cosmology was equal to the true cosmology.

Alcock–Paczynski methodology to the WiggleZ survey clustering by measuring the relative amplitude of the power spectrum modes as a function of their angle to the line of sight (Ballinger et al. 1996; Matsubara & Suto 1996; Simpson & Peacock 2010), assuming the underlying isotropy of these modes in the true cosmological model.

In more detail, the true values of the angular diameter distance $D_A(z)$ and Hubble expansion parameter $H(z)$ may differ from our adopted fiducial values, $\hat{D}_A(z)$ and $\hat{H}(z)$, leading to two scaling factors, $f_\perp \equiv D_A/\hat{D}_A$ and $f_\parallel \equiv \hat{H}/H$, which relate the apparent, observed tangential and radial wavenumber components $(k'_\perp, k'_\parallel)$ to their true values $(k_\perp, k_\parallel)$ via $k'_\perp = f_\perp k_\perp$ and $k'_\parallel = f_\parallel k_\parallel$. The apparent two-dimensional galaxy power spectrum is then related to the underlying fiducial galaxy power spectrum (ignoring redshift-space distortions for the moment) by

$$P_g(k', \mu') = \frac{b^2}{f_\perp^2 f_\parallel} P_m \left[\frac{k'}{f_\perp} \sqrt{1 + \mu'^2 \left(\frac{f_\perp^2}{f_\parallel^2} - 1 \right)} \right] \quad (2)$$

(following Ballinger et al. 1996; Simpson & Peacock 2010), where $k' = \sqrt{k_\perp'^2 + k_\parallel'^2}$, $\mu' = k'_\parallel/k'$, b is an unknown galaxy bias factor, and $P_m(k)$ is the underlying real-space, isotropic matter power spectrum. We generated this power spectrum shape using the CAMB software (Lewis, Challinor & Lasenby 2000) with cosmological parameters consistent with the latest observations of the CMB radiation (Komatsu et al. 2011): matter density $\Omega_m = 0.27$, cosmological constant $\Omega_\Lambda = 0.73$, baryon fraction $\Omega_b/\Omega_m = 0.166$, Hubble parameter $h = 0.71$, primordial scalar index of fluctuations $n_s = 0.96$

and total fluctuation amplitude $\sigma_8 = 0.8$. We included non-linear growth of structure in this model using the 'halofit' prescription in CAMB (Smith et al. 2003). These assumptions do not introduce a significant model dependence in our analysis, as discussed in Section 3.4.

If the underlying power spectrum $P_m(k)$ contains features at known physical scales, which we can clearly detect as a function of angle, then we can extract both the distortion factors $(f_\parallel, f_\perp)$. This would be equivalent to knowing the absolute length-scale L_0 introduced above, and may be achieved in principle using baryon acoustic oscillations as a standard ruler (Hu & Haiman 2003; Seo & Eisenstein 2003; Glazebrook & Blake 2005). However, the 2D WiggleZ power spectra do not possess a sufficiently high signal-to-noise ratio to resolve the imprint of baryon oscillations.

If the power spectrum can be well approximated by a scale-free power law over the range of the scales of interest, which is a valid approximation here, then we have no knowledge of L_0 and can only measure $f_\parallel/f_\perp = D_A(z)H(z)/\hat{D}_A(z)\hat{H}(z) = F/F_{\text{fid}}$, where F is the observed scale distortion factor and F_{fid} is its value in the fiducial model. This situation corresponds to the Alcock–Paczynski measurement [note that any constants of proportionality in the power spectrum on the right-hand side of equation (2) are absorbed into the unknown bias factor b]. In our default implementation for determining the best-fitting value of F, we varied the value of $f_\perp = F_{\text{fid}}/F$ and fixed $f_\parallel = 1$. We checked that our results were not significantly changed if we instead varied $f_\parallel = F/F_{\text{fid}}$, fixing $f_\perp = 1$, or varied both $f_\perp = \sqrt{F_{\text{fid}}/F}$ and $f_\parallel = \sqrt{F/F_{\text{fid}}}$.

3.2 Redshift-space distortion models

The application of the Alcock–Paczynski measurement to large-scale galaxy clustering is complicated by the fact that there is a second physical cause of anisotropy in the observed 'redshift space': the coherent, bulk flows of galaxies towards clusters and superclusters that induce systematic offsets in galaxy redshifts and hence produce a radial (but not tangential) power spectrum distortion (Kaiser 1987; Hamilton 1992). In other words, the redshift-space clustering pattern is not isotropic in the true cosmological model.

Under a set of general assumptions, independently of the cosmic expansion history and the Friedmann–Robertson–Walker (FRW) metric, the redshift-space power spectrum of a population of galaxies may be written as

$$P_g^s(k, \mu) = P_{gg}(k) - 2\mu^2 P_{g\theta}(k) + \mu^4 P_{\theta\theta}(k), \tag{3}$$

where $P_{gg}(k) \equiv \langle |\delta_g(\boldsymbol{k})|^2 \rangle$, $P_{g\theta}(k) \equiv \langle \delta_g(\boldsymbol{k}) \theta^*(\boldsymbol{k}) \rangle$ and $P_{\theta\theta}(k) \equiv \langle |\theta(\boldsymbol{k})|^2 \rangle$ are the isotropic galaxy–galaxy, galaxy–velocity and velocity–velocity power spectra (e.g. Samushia et al. 2011). These equations are given in terms of $\delta_g(\boldsymbol{k})$, the Fourier transform of the galaxy overdensity field, and $\theta(\boldsymbol{k})$, the Fourier transform of the divergence of the peculiar velocity field in the unit of the comoving Hubble velocity (Percival & White 2009).

We assume a linear bias factor b relating the large-scale galaxy overdensity δ_g to the underlying matter overdensity δ predicted by theory: $\delta_g = b\,\delta$. In this case $P_{gg} = b^2 P_{\delta\delta}$ and $P_{g\theta} = b\,P_{\delta\theta}$. Blake et al. (2011a) have shown that WiggleZ galaxies follow a distribution that closely matches the underlying matter ($b \approx 1$), and that the galaxy–mass cross-correlation is consistent with a deterministic, linear bias over the range of scales relevant for this analysis.

In the linear perturbation theory in an FRW metric, the application of the continuity equation implies that $P_{\delta\delta} = -f\,P_{\delta\theta} = f^2\,P_{\theta\theta}$, where f is the growth rate of structure, expressible in terms of the growth factor $D(a)$ at cosmic scalefactor a as $f \equiv \mathrm{d}\ln D / \mathrm{d}\ln a$, where the growth factor describes the evolution of the amplitude of a single perturbation, $\delta(a) = D(a)\,\delta(1)$. In this case we recover the large-scale 'Kaiser limit' (Kaiser 1987):

$$P_g^s(k, \mu) = b^2\,P_{\delta\delta}(k)\,(1 + \beta\,\mu^2)^2, \tag{4}$$

where $\beta = f/b$. In this approximation, equation (2) can be modified to include redshift-space distortions as

$$
\begin{aligned}
P_g^s(k', \mu') = {} & \frac{b^2}{f_\perp^2 f_\parallel} \left[1 + \mu'^2 \left(\frac{1+\beta}{F^2/F_{\text{fid}}^2} - 1 \right) \right]^2 \\
& \times \left[1 + \mu'^2 \left(\frac{F_{\text{fid}}^2}{F^2} - 1 \right) \right]^{-2} \\
& \times P_m \left[\frac{k'}{f_\perp} \sqrt{1 + \mu'^2 \left(\frac{F_{\text{fid}}^2}{F^2} - 1 \right)} \right]
\end{aligned}
\tag{5}
$$

(following Ballinger et al. 1996; Simpson & Peacock 2010). Although there is some degeneracy between β and the Alcock–Paczynski distortion parameter F, their angular signatures in the clustering model are sufficiently different that both parameters may be successfully extracted after marginalizing over the other.

However, *we do not use the redshift-space distortion model of equation (5) in our default analysis* because the Kaiser-limit approximation is only appropriate at the largest scales (lowest values of k) due to the non-linear growth of structure at smaller scales (Jennings, Baugh & Pascoli 2011; Okumura & Jing 2011). As a result, fitting equation (5) to the galaxy power spectra could produce a systematic error in the recovered values of F and β; we include

the equations simply to illustrate how F and β may be disentangled in model-fitting.

The signature of redshift-space distortions has been modelled in more detail by many authors using various techniques including empirical fitting formulae (Hatton & Cole 1998), numerical N-body dark matter simulations (Jennings et al. 2011) and perturbation theory (Crocce & Scoccimarro 2006; Taruya, Nishimichi & Saito 2010). A full comparison of WiggleZ clustering data to these models was presented by Blake et al. (2011a).

In the current study, we took as our fiducial redshift-space distortion model the fitting formulae provided by Jennings et al. (2011), which allow us to generate the functions $P_{\delta\theta}(k)$ and $P_{\theta\theta}(k)$ in equation (3) for given values of the growth rate f and the non-linear matter power spectrum $P_{\delta\delta}(k) = P_m(k)$ (which we obtained using 'halofit' in CAMB). The Jennings et al. (2011) formulae have been constructed to be valid for a range of physical dark energy models, and they do not pre-suppose any specific continuity equation linking velocity and density. Unlike the Kaiser limit they do not assume an FRW metric, as discussed by Samushia et al. (2011). We consider the effect of different choices of the redshift-space distortion model in Section 3.4.

As a further enhancement of the redshift-space distortion model, we also considered multiplying equation (3) by an empirical damping function $D(k, \mu)$, representing convolution with uncorrelated galaxy motions on small scales. The standard choice for this damping function is a Lorentzian $D(k, \mu) = [1 + (k_\parallel \sigma_v)^2]^{-1}$, where σ_v is the pairwise velocity dispersion, which may be varied as a free parameter but is set to zero for our default model. The effects of this choice on the Alcock–Paczynski measurements are considered in Section 3.4.

3.3 Model fits

We fitted our default Jennings et al. (2011) clustering model, parametrized by (F, f, b^2), to the WiggleZ Survey power spectra over the range of scales $k < 0.2\,h\,\mathrm{Mpc}^{-1}$. Fig. 2 displays the joint likelihoods of the scale distortion parameter and growth rate in each of the redshift slices. We quantify the growth rate in this figure by $f\sigma_8(z)$, where $\sigma_8(z) = D(z)\sigma_8(0)$ quantifies the normalization of the matter power spectrum at redshift z. This is a more model-insensitive observable than the growth rate itself owing to the degeneracy between $\sigma_8(z)$ and the galaxy bias b in determining the overall galaxy clustering amplitude. We note that there is a strong correlation between F and $f\sigma_8$, with correlation coefficients $r = (0.83, 0.94, 0.89, 0.84)$ in the four redshift slices, but both parameters may be successfully extracted. The marginalized measurements of the growth rate are $f\sigma_8(z) = (0.53 \pm 0.14, 0.40 \pm 0.13, 0.37 \pm 0.08, 0.49 \pm 0.12)$. These measurements are consistent with those reported by Blake et al. (2011a) who considered fits of redshift-space distortion models assuming $F = F_{\text{fid}}$. The resulting measurements of F, marginalizing over f and b^2, are plotted in Fig. 3 as solid black data points. Our result is $F(z) \equiv (1 + z)D_A(z)H(z)/c = (0.28 \pm 0.04, 0.44 \pm 0.07, 0.68 \pm 0.06, 0.97 \pm 0.12)$ in the four redshift slices. All of the different measurements reported in Sections 3, 4 and 5 are brought together in Table 1 for convenience.

3.4 Systematics tests

Fig. 3 presents some tests of the sensitivity of our results to the different assumptions in the model described above. First, we checked that our measurement of F did not significantly change if we replaced our default model with a range of other implementations
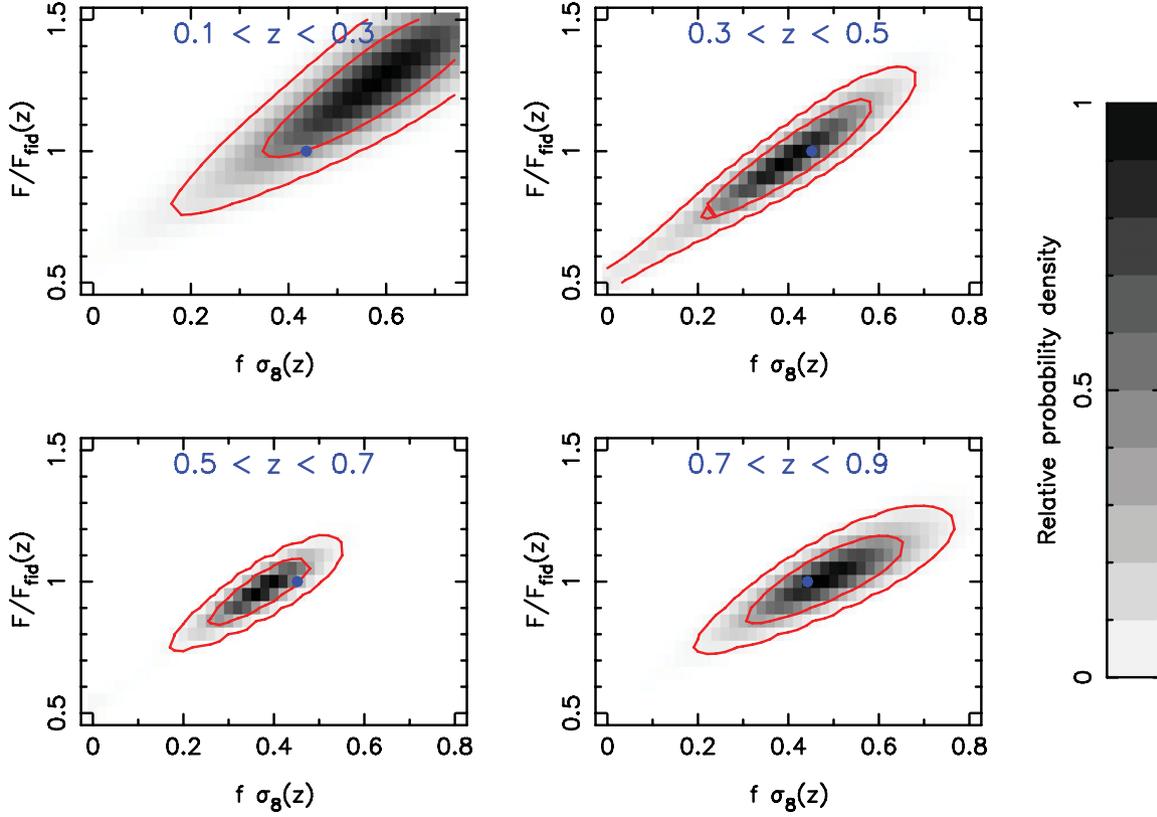
Figure 2. This figure displays the joint likelihood of the Alcock–Paczynski scale distortion parameter $F(z)$ relative to the fiducial value F_{fid}, and the growth rate quantified by $f\sigma_8(z)$, obtained from fits to the 2D galaxy power spectra of the WiggleZ Dark Energy Survey in four redshift slices. In order to produce this figure we marginalized over the linear galaxy bias b^2 and the pairwise velocity dispersion σ_v. There is some degeneracy between F and $f\sigma_8$ but their characteristic dependence on the angle to the line of sight is sufficiently different that both parameters may be successfully extracted. The probability density is plotted as both grey-scale and contours enclosing 68 and 95 per cent of the total likelihood. The solid circles indicate the parameter values in our fiducial cosmological model.

Table 1. This table brings together the results of the various cosmological model fits to the galaxy clustering via the Alcock–Paczynski (AP) measurement and supernovae (SNe) data presented in this study. Results are presented for four different redshift slices.

Statistic	Method	$0.1 < z < 0.3$	$0.3 < z < 0.5$	$0.5 < z < 0.7$	$0.7 < z < 0.9$
Effective redshift z		0.22	0.41	0.60	0.78
$F_{fid}(z)$		0.23	0.46	0.71	0.97
$F(z) \equiv (1+z)D_A(z)H(z)/c$	AP fit	0.28 ± 0.04	0.44 ± 0.07	0.68 ± 0.06	0.97 ± 0.12
$f\sigma_8(z)$	AP fit	0.53 ± 0.14	0.40 ± 0.13	0.37 ± 0.08	0.49 ± 0.12
Cross-correlation in $(F, f\sigma_8)$	AP fit	0.83	0.94	0.89	0.84
$D_A(z)H_0/c$	SN fit	0.210 ± 0.001	0.376 ± 0.005	0.526 ± 0.010	0.655 ± 0.015
$D_A(z)H_0/c$	Reconstruction	0.209 ± 0.001	0.371 ± 0.003	0.517 ± 0.006	0.652 ± 0.012
$H(z)/[H_0(1+z)]$	AP + SN fit	1.11 ± 0.17	0.83 ± 0.13	0.81 ± 0.08	0.83 ± 0.10
$H(z)/[H_0(1+z)]$	Reconstruction	0.91 ± 0.02	0.88 ± 0.03	0.88 ± 0.08	0.80 ± 0.08
$Om(z)$	Reconstruction	0.28 ± 0.05	0.29 ± 0.07	0.31 ± 0.13	0.22 ± 0.09
$q(z)$	Reconstruction	-0.3 ± 0.2	-0.8 ± 0.9	-1.2 ± 2.0	6.4 ± 4.9

of redshift-space distortions discussed in recent literature, including generating the density and velocity power spectra using the renormalized perturbation theory (Crocce & Scoccimarro 2006) and adding the correction terms proposed by Taruya et al. (2010). Indeed, using the simplification of equation (5), where $P_{\delta\delta}(k)$ is the non-linear power spectrum obtained from CAMB, produced an unchanged result for F (within the statistical errors), as illustrated in Fig. 3 (the cyan data points).

We also considered including and excluding the pairwise velocity dispersion as a free parameter. If we fit for F by varying $f_{\perp}$ and fixing $f_{\parallel}$, then marginalizing over the additional free parameter σ_v makes

no difference to our results (illustrated by the blue data points in Fig. 3). However, if we fit for F by varying $f_{\parallel}$ and fixing $f_{\perp}$ then the resulting error in F significantly increases by marginalizing over σ_v, due to the cross-talk between $k_{\parallel}$ and σ_v in the damping term.

Any potential systematic error in the redshift-space distortion model is likely to worsen at smaller scales (higher values of k) where the modelling becomes less accurate. We carefully compared different choices of the fitting range $0 < k < k_{max}$ in order to ensure that any systematic error in the derived distortion parameter was not significant. The results of some of these tests are plotted in Fig. 3. Our fiducial choice, $k_{max} = 0.2\,h\,\mathrm{Mpc}^{-1}$, was determined
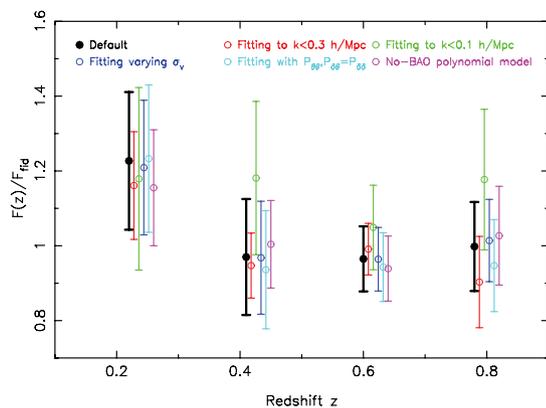
Figure 3. This figure quantifies the amplitude of systematic errors in our measurements of the scale distortion parameter $F(z)$ in four redshift slices relative to the fiducial value F_{fid}, marginalized over the growth rate f, galaxy bias b^2 and pairwise velocity dispersion σ_{v} (where appropriate). The solid black data points show our default measurement using the redshift-space distortion model provided by Jennings et al. (2011) fitting to the wavenumber range $0 < k < k_{\max} = 0.2\,h\,\text{Mpc}^{-1}$. The remaining data points illustrate the effects of varying these assumptions: using $k_{\max} = 0.3\,h\,\text{Mpc}^{-1}$ (red), $k_{\max} = 0.1\,h\,\text{Mpc}^{-1}$ (green), adding the pairwise velocity dispersion as a free parameter (blue), fitting using the large-scale Kaiser limit formula of equation (5) (cyan), and using the data themselves to define the real-space power spectrum via a polynomial fit to an angle-averaged measurement of $P(k)$ (magenta). Each subsequent data point is slightly offset in redshift for clarity.

by the consideration that the measurements of F should not differ systematically between different implementations of the redshift-space distortion model. Results for $k_{\max} = 0.1$ and $0.3\,h\,\text{Mpc}^{-1}$ are displayed as the red and green data points in Fig. 3. As a further test we repeated the measurements of F for independent scale ranges $k = 0$–0.1, 0.1–0.2 and 0.2–$0.3\,h\,\text{Mpc}^{-1}$; the results were consistent within the statistical errors.

Our analysis uses an underlying isotropic matter power spectrum that is consistent with the latest observations of the CMB radiation (Komatsu et al. 2011). In order to show that this does not introduce any sensitivity to the model into our analysis, we checked that our results were unchanged if we instead generated a function proportional to $P_{\text{m}}(k)$ using a polynomial fit to the observed, angle-averaged galaxy power spectrum in the fiducial model; this comparison is shown as the magenta data points in Fig. 3. The similarity between these measurements and our fiducial results is further evidence that the baryon acoustic oscillations (which do not appear in a smooth polynomial model) are not contributing any information to the Alcock–Paczynski distortion fits.

We conclude from these tests that the systematic error in F induced from modelling redshift-space distortions is much lower than the statistical error in the measurement. We therefore refer to our results as 'model-insensitive' (to first order), even though a series of model assumptions are necessary to produce these fits.

4 DETERMINATION OF THE COSMIC EXPANSION HISTORY

We converted our Alcock–Paczynski measurements of the scale distortion parameter $F(z) = (1 + z)D_{\text{A}}(z)H(z)/c$ into a determination of the cosmic expansion history $H(z)$ by using Type Ia supernovae (SNe Ia) data to fix the cosmic distance–redshift relation. We used the 'Union-2' compilation by Amanullah et al. (2010) as our SNe data set, obtained from the web site http://supernova.lbl.gov/Union.
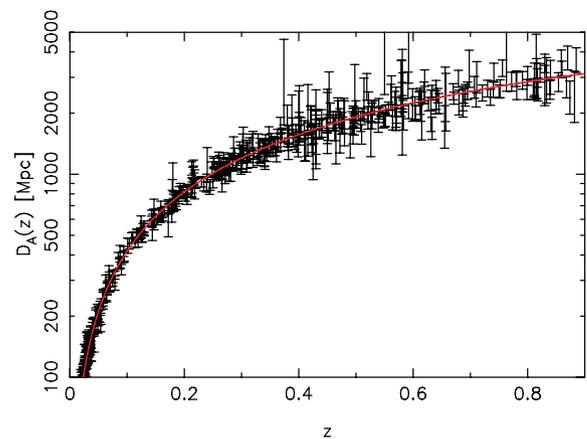

Figure 4. This figure displays the best-fitting third-order polynomial to the Union-2 compilation of supernovae data, normalized as a plot of angular-diameter distance versus redshift.

This compilation of 557 SNe includes data from Hamuy et al. (1996), Riess et al. (1999, 2007), Astier et al. (2006), Jha et al. (2006), Wood-Vasey et al. (2007), Holtzman et al. (2008), Hicken et al. (2009) and Kessler et al. (2009).

Given that the normalization of the SN *Hubble* diagram M–$5\log_{10}h$ is treated as an unknown parameter, the SNe data yield the relative luminosity distance $D_{\text{L}}(z)\,H_0/c$. We determined a model-insensitive value of this quantity in each redshift slice by fitting the distance–redshift relation as a third-order polynomial in z (over the redshift range $0 < z < 0.9$) and marginalizing over the values of the polynomial coefficients. We used the full covariance matrix of the SNe measurements including systematic errors, and checked that our results were not significantly changed by assuming a second-order or fourth-order polynomial instead. Our results at the four redshifts $z = (0.22, 0.41, 0.6, 0.78)$ were $D_{\text{A}}(z)\,H_0/c = (0.210 \pm 0.001, 0.376 \pm 0.005, 0.526 \pm 0.010, 0.655 \pm 0.015)$, where we converted the luminosity distances to angular diameter distances assuming $D_{\text{L}}(z) = D_{\text{A}}(z)(1 + z)^2$. We note that the inclusion of the SNe systematics covariance matrix (compared to uncorrelated errors excluding systematics) increases the errors in these measurements of $D_{\text{A}}\,H_0/c$ by a factor of 2. The SNe data points and the best-fitting third-order polynomial model are displayed in Fig. 4. This model provides a good fit to the data, with a chi-squared statistic of 486.6 for 519 degrees of freedom.

Combining the Alcock–Paczynski and SNe measurements in the four redshift slices, we find that $H(z)/[H_0(1+z)] \equiv \dot{a}/\dot{a}_0 = (1.11 \pm 0.17, 0.83 \pm 0.13, 0.81 \pm 0.08, 0.83 \pm 0.10)$, where $\dot{a}_0 \equiv H_0$. These results are plotted as the black error bars in Fig. 5 and compared to three expansion history models: a ΛCDM cosmology with matter density $\Omega_{\text{m}} = 0.27$, an Einstein–de Sitter (EdS) model with $\Omega_{\text{m}} = 1$ and a 'coasting' model for which $\text{d}a/\text{d}t = H_0$ at all times. We find that our measurements are consistent with the ΛCDM model. Fig. 5 constitutes our model-insensitive measurement of the cosmic expansion rate $\text{d}a/\text{d}t$, with 10–15 per cent precision in each of the four redshift slices. We note that the systematic errors in the SNe measurements are insignificant in the determination of $H(z)/[H_0(1 + z)]$ because the error propagation is dominated by the error in the Alcock–Paczynski measurement.

An accelerating expansion implies a decrease in the value of $\text{d}a/\text{d}t$ with an increasing redshift. This is directly observed in our data: if we fit the data for a constant value of $\dot{a}/\dot{a}_0$, we find that the range $\dot{a}/\dot{a}_0 < 1$, containing accelerating-expansion models,
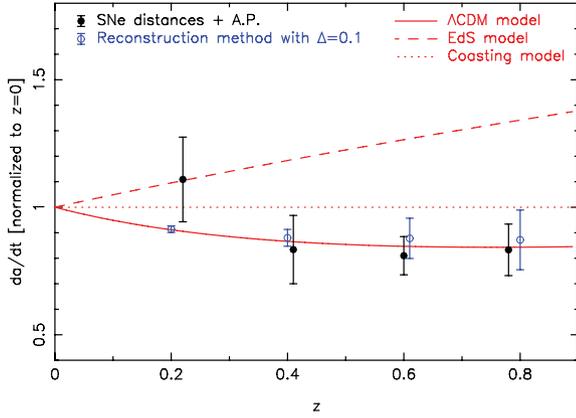
Figure 5. This figure displays our measurement of the evolution of the cosmic expansion rate using Alcock–Paczynski and supernovae data. The expansion rate is displayed using the value of $\dot{a}/\dot{a}_0 = H(z)/[H_0(1 + z)]$; accelerating expansion implies a decrease in the value of this quantity with increasing redshift. The black data points (solid circles) are obtained by combining Alcock–Paczynski measurements of $(1 + z)D_A(z)H(z)/c$ in four independent redshift slices with supernovae distance determinations of $D_L(z)H_0/c$ at these redshifts, and are independent of curvature. The blue data points (open circles) result from applying the distance reconstruction method of Shafieloo et al. (2006) to both the supernovae and Alcock–Paczynski data, producing optimal errors at both low and high redshift but making the additional assumptions of zero spatial curvature and that $D_A(z)$ may be expressed in terms of an integral over $1/H(z)$. Predictions are plotted for three different models: a fiducial ΛCDM model with $\Omega_m = 0.27$ (solid line), an Einstein–de Sitter model with $\Omega_m = 1$ (dashed line), and a 'coasting' model where $\dot{a} = $ constant (dotted line).

contains 99.86 per cent of the probability. Hence in this assessment, accelerating-expansion models are preferred with a statistical significance of more than 3σ. We stress that this is a model-insensitive, non-parametric result based solely on combining Alcock–Paczynski measurements of $D_A(z)H(z)$ with the SNe measurements of $D_A(z)$.

5 FULL DISTANCE–REDSHIFT RECONSTRUCTION

In this section we use our data sets to map out the full cosmic expansion history via the non-parametric reconstruction method introduced by Shafieloo et al. (2006). We note that, unlike the preceding analysis, this approach assumes zero spatial curvature and that $D_A(z)$ can be expressed in terms of an integral over $1/H(z)$ (i.e. the FRW metric). Hence we expect to derive tighter constraints based on more assumptions.

5.1 Method for reconstructing $D_A(z)$

We first describe the application of the Shafieloo et al. (2006) distance reconstruction method to SNe Ia data. We then outline its generalization to enable the inclusion of the Alcock–Paczynski measurements.

The methodology of Shafieloo et al. (2006) is an iterative approach that deduces a distance–redshift curve $D_A(z)$ from an initial guess model by smoothing the residuals between the model and measurements of $D_A(z)$ and using these residuals to modify the guess. Iteration proceeds until the chi-squared statistic between model and data is minimized. The only parameter required by the method is the width of the smoothing kernel in redshift, Δ (our fiducial value is $\Delta = 0.1$, other choices are considered below). For the initial guess model to commence the iteration, we chose a flat

ΛCDM model with $\Omega_m = 0.27$. Our results have no sensitivity to the choice of initial guess (as illustrated by the offset between the reconstructed and fiducial distance curve in the top left-hand panel of Fig. 6). We defined the model on a grid of redshift steps spaced by $dz = 0.01$ from $z = 0$–1.

The equation generating iteration $i + 1$ from iteration i, in terms of the SNe data points j, is given in Shafieloo & Clarkson (2010):

$$\ln D_L(z)^{i+1} = \ln D_L(z)^i + N(z)$$
$$\times \sum_j \frac{[\ln D_L(z_j) - \ln D_L(z_j)^i]}{\sigma_j^2} \exp\left[-\frac{(z_j - z)^2}{2\Delta^2}\right],$$
(6)

where the redshift-dependent normalization is

$$N(z)^{-1} = \sum_j \frac{1}{\sigma_j^2} \exp\left[-\frac{(z_j - z)^2}{2\Delta^2}\right].$$
(7)

For the inverse-variance weighting σ_j, we followed Shafieloo & Clarkson (2010) and used the error in each SN luminosity distance.

We then modified the distance reconstruction method to utilize the residuals with respect to the Alcock–Paczynski data points. We initially generated an iterative correction to the quantity $F(z) = (1 + z)D_A(z)H(z)/c$ using an analogous method to equation (6):

$$\Delta F(z) = M(z) \sum_k \frac{F(z_k) - F(z_k)^i}{\sigma_k^2} \exp\left[-\frac{(z_k - z)^2}{2\Delta^2}\right],$$
(8)

where k labels the Alcock–Paczynski measurements at redshifts z_k, with errors σ_k in $F(z)$, and the normalization factor is given by

$$M(z)^{-1} = \sum_k \frac{1}{\sigma_k^2} \exp\left[-\frac{(z_k - z)^2}{2\Delta^2}\right].$$
(9)

We then converted the iteration in $F(z)$ into an iteration in $D_L(z) = (1 + z)^2 D_A(z)$ using

$$D_A(z)^{i+1} = D_A(z)^i$$
$$- \sum_{z'}(1 + z')D_A(z')^i \frac{\Delta F(z')}{[F(z')^i]^2}\Delta z',$$
(10)

where $\Delta z' = 0.01$ is the redshift interval of the gridding of the model curves. The right-hand side of equation (10) is derived by expressing $D_A(z) = \sum_{z'}[c/H(z')]\Delta z'$, substituting $c/H(z') = (1 + z')D_A(z')/F(z')$, and taking the derivative with respect to F. At each step in the iteration we applied the residual distance correction for both the SNe and Alcock–Paczynski data points, proceeding until the chi-squared statistic was minimized.

We estimated the error in the distance–redshift reconstruction by repeating the iterative process using bootstrap resamples of the data sets. The range of resulting distance–redshift curves across the resamples defines the error in the reconstruction. We performed extensive tests using Monte Carlo realizations of synthetic data sets to verify that this procedure produced bias-free reconstructions with reliable error ranges. We note that this procedure differs from that of Shafieloo et al. (2006) and Shafieloo & Clarkson (2010), who used the set of distance curves $[\ln D_L(z)^i]$ generated by a single application of the iteration process of equation (6) to estimate the error in the reconstruction. In order to obtain the error in the reconstructed curves we constructed separate bootstrap resamples of the SNe and Alcock–Paczynski data points.

5.2 Method for reconstructing $H(z)$, $Om(z)$ and $q(z)$

We used the reconstructed distance–redshift curves to determine three other diagnostics that describe the cosmic expansion history.
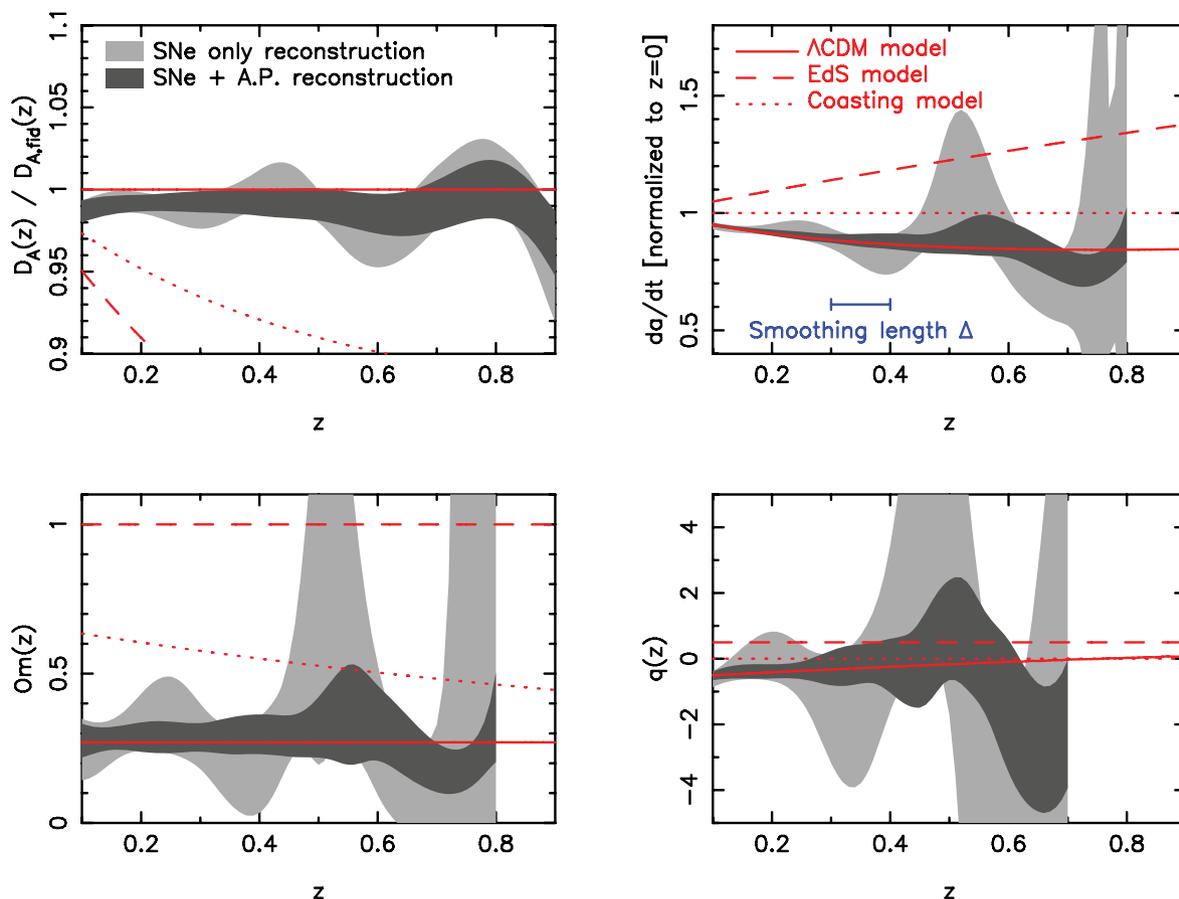
Figure 6. This figure shows our non-parametric reconstruction of the cosmic expansion history using Alcock–Paczynski and supernovae data. The four panels of this figure display our reconstructions of the distance–redshift relation $D_A(z)$, the expansion rate $\dot{a}/H_0$, the Om(z) statistic and the deceleration parameter $q(z)$ using our adaptation of the iterative method of Shafieloo et al. (2006) and Shafieloo & Clarkson (2010). The distance–redshift relation in the upper left-hand panel is divided by a fiducial model for clarity, where the model corresponds to a flat ΛCDM cosmology with $\Omega_m = 0.27$. This fiducial model is shown as the solid line in all panels; Einstein–de Sitter and coasting models are also shown, defined as they are in Fig. 5. The shaded regions illustrate the 68 per cent confidence range of the reconstructions of each quantity obtained using bootstrap resamples of the data. The dark-grey regions utilize a combination of the Alcock–Paczynski and supernovae data and the light-grey regions are based on the supernovae data alone. The redshift smoothing scale $\Delta = 0.1$ is also illustrated. The reconstructions in each case are terminated when the SNe-only results become very noisy; this maximum redshift reduces with each subsequent derivative of the distance–redshift relation [i.e. is lowest for $q(z)$].

First, assuming a flat Universe we can differentiate the reconstructed distance–redshift curves to determine the expansion rate $\dot{a}/\dot{a}_0 = H(z)/[H_0(1 + z)]$. Secondly, a useful diagnostic of the expansion history that can be derived from $H(z)$ is the 'Om' statistic (Sahni, Shafieloo & Starobinsky 2008):

$$\text{Om}(z) \equiv \frac{[H(z)/H_0]^2 - 1}{(1 + z)^3 - 1}. \tag{11}$$

In a spatially flat ΛCDM model this statistic is constant at different redshifts and equal to today's value of the matter density parameter Ω_m. In universes with different curvature, or containing dark energy with different properties to a cosmological constant, Om(z) would evolve with redshift. Finally, by a second differentiation of the distance–redshift curves, we can obtain the deceleration parameter $q(z) \equiv -\ddot{a}a/\dot{a}^2$:

$$q(z) = (1 + z)\frac{\mathrm{d}H(z)/\mathrm{d}z}{H(z)} - 1. \tag{12}$$

The confidence ranges for the reconstruction of each quantity are established using bootstrap resampling.

5.3 Results of the reconstruction

Fig. 6 displays our non-parametric reconstructions of the four quantities $D_A(z)$, da/dt, Om(z) and $q(z)$. The light-grey regions display the 68 per cent confidence range of reconstructions using the SNe data alone, and the inner dark-grey region derives from the combination of SNe and Alcock–Paczynski measurements.

The addition of the Alcock–Paczynski data does not strongly enhance the reconstruction of the distance–redshift relation $D_A(z)$, which is very well measured by SNe alone. However, the direct sensitivity of $F(z)$ to $H(z)$ produces dramatic improvements in the reconstruction of the expansion-rate history, with a factor of 3 shrinking of the confidence ranges in $H(z)$ for $z > 0.2$. At the four redshifts $z = (0.22, 0.41, 0.6, 0.78)$, the reconstruction method gives us $H(z)/[H_0(1 + z)] = (0.91 \pm 0.02, 0.88 \pm 0.03, 0.88 \pm 0.08, 0.80 \pm 0.08)$. These measurements are correlated, but the level of correlation is low because the fiducial choice of the smoothing length $\Delta = 0.1$ is somewhat smaller than the binwidth $\Delta z = 0.2$.

Our measurements establish the constancy of Om(z) with redshift for the first time with reasonable precision, a key prediction of a flat ΛCDM model. At the four redshifts listed above the reconstruction method produces Om(z) = $(0.28 \pm 0.05, 0.29 \pm 0.07, 0.31 \pm$
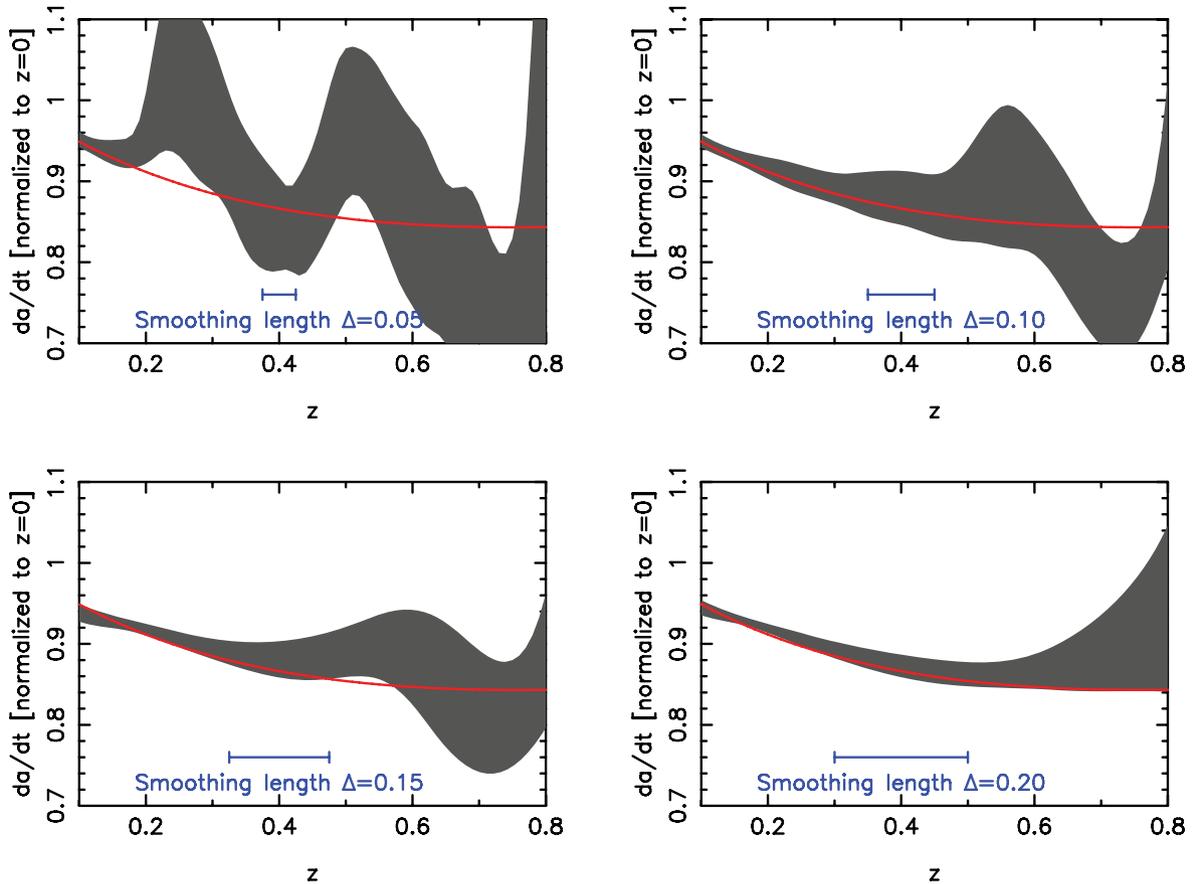
Figure 7. In this figure we repeat the reconstruction of $\dot{a}/H_0$ using both supernovae and Alcock–Paczynski data for different choices of the smoothing length Δ, the only free parameter in the reconstruction algorithm. The solid band shows the 68 per cent confidence range spanned by the reconstructions, and the solid red line is the prediction of a flat ΛCDM model with $\Omega_m = 0.27$.

$0.13, 0.22 \pm 0.09$). If we fit these values for the matter density in a flat ΛCDM model, we find $\Omega_m = 0.29 \pm 0.03$, consistent with fits to the CMB radiation (Komatsu et al. 2011).

We also overplot in Fig. 5 the non-parametric measurements of $\mathrm{d}a/\mathrm{d}t$ obtained by this reconstruction method in the four redshift slices. A comparison of the errors with the direct combination of SNe distances and Alcock–Paczynski data shows that at low redshifts the SNe data alone place the most powerful constraint on the expansion history, greatly improving the results presented in Section 4, but at higher redshifts the Alcock–Paczynski data are crucial in order to obtain accurate measurements.

Fig. 7 illustrates the effect of changing the smoothing length on the reconstructed expansion history $\dot{a}/\dot{a}_0$, considering the values $\Delta = 0.05, 0.10, 0.15$ and 0.20. A flat ΛCDM model with $\Omega_m = 0.27$, shown as the solid line, continues to be a good description of the expansion history regardless of the smoothing scale. We checked that the error in fitting Ω_m to these data was insensitive to Δ when covariances between different redshifts were taken into account (estimating these covariances using the bootstrap resamples).

6 CONCLUSIONS

We summarize our study as follows.

(i) We have performed joint fits for the Alcock–Paczynski scale distortion parameter $F(z) = (1 + z)D_A(z)H(z)/c$ and the normalized growth rate $f\sigma_8(z)$, using 2D power spectra measured from the WiggleZ Dark Energy Survey in four redshift bins in the range $0.1 <$

$z < 0.9$. We can separate the contributions of Alcock–Paczynski and redshift-space distortions, and our result is insensitive to the range of models we examined for non-linear redshift-space effects when fitted to the wavenumber range $k < 0.2\,h\,\mathrm{Mpc}^{-1}$.

(ii) By combining the Alcock–Paczynski fits with luminosity–distance measurements using Type Ia SNe, we determined the cosmic expansion rate $\dot{a}/\dot{a}_0 = H(z)/[H_0(1+z)]$ in four redshift slices with 10–15 per cent accuracy. Our results for redshifts $z = (0.22, 0.41, 0.6, 0.78)$ are $\dot{a}/\dot{a}_0 = (1.11 \pm 0.17, 0.83 \pm 0.13, 0.81 \pm 0.08, 0.83 \pm 0.10)$. These measurements are independent of spatial curvature.

(iii) Our measurements show that the value of $\dot{a}$ was lower at high redshifts, demonstrating that the cosmic expansion has accelerated. If we fit for a constant value of $\dot{a}$ in the redshift range $0.1 < z < 0.9$, we find that accelerating-expansion models are favoured with a statistical significance of more than 3σ.

(iv) We used an adapted version of the reconstruction method of Shafieloo et al. (2006) to model the continuous cosmic expansion history since $z = 0.9$ using both the Alcock–Paczynski and SNe data sets. The Alcock–Paczynski measurements enable a much more accurate determination of the expansion history than the SNe data alone. We demonstrate that the quantity $\mathrm{Om}(z) \equiv \{[H(z)/H_0]^2 - 1\}/[(1 + z)^3 - 1]$ is constant with redshift, as expected in a spatially flat ΛCDM model; fitting for the value of this quantity allows us to obtain an estimate of the matter-density parameter $\Omega_m = 0.29 \pm 0.03$, consistent with fits to the CMB radiation (Komatsu et al. 2011).

We conclude that accelerating cosmic expansion can be recovered from cosmological data in a non-parametric and model-insensitive manner and hence it is a real physical phenomenon that must be accounted for by theory. The measured expansion history is well fitted by a cosmological constant which grows in relative importance with cosmic time. The combination of Alcock–Paczynski and SNe data is a novel approach that enables direct observation of the Hubble expansion rate and will be strengthened in the future by the availability of new galaxy redshift survey data.

REFERENCES

Alcock C., Paczynski B., 1979, Nat, 281, 358
Amanullah R. et al., 2010, ApJ, 716, 712
Astier P. et al., 2006, A&A, 447, 31
Ballinger W. E., Peacock J. A., Heavens A. F., 1996, MNRAS, 282, 877
Blake C. A. et al., 2010, MNRAS, 406, 803
Blake C. A. et al., 2011a, MNRAS, 415, 2876
Blake C. A. et al., 2011b, MNRAS, 415, 2892
Chuang C.-H., Wang Y., 2011, preprint (arXiv:1102.2251)
Conley A. et al., 2011, ApJS, 192, 1
Crocce M., Scoccimarro R., 2006, Phys. Rev. D, 73, 3519
Drinkwater M. et al., 2010, MNRAS, 401, 1429
Eisenstein D. J. et al., 2011, AJ, 142, 72
Feldman H. A., Kaiser N., Peacock J. A., 1994, ApJ, 426, 23
Gaztanaga E., Cabre A., Hui L., 2009, MNRAS, 399, 1663
Giannantonio T. et al., 2008, Phys. Rev. D, 77, 3520
Gilbank D. G., Gladders M. G., Yee H. K. C., Hsieh B. C., 2011, AJ, 141, 94

Glazebrook K., Blake C. A., 2005, ApJ, 631, 1
Hamilton A. J. S., 1992, ApJ, 385, 5
Hamuy M. et al., 1996, AJ, 112, 2408
Hatton S., Cole S., 1998, MNRAS, 296, 10
Hicken M. et al., 2009, ApJ, 700, 331
Holtzman J. A. et al., 2008, AJ, 136, 2306
Hu W., Haiman Z., 2003, Phys. Rev. D, 68, 63004
Jennings E., Baugh C. M., Pascoli S., 2011, MNRAS, 410, 2081
Jha S. et al., 2006, AJ, 131, 527
Kaiser N., 1987, MNRAS, 227, 1
Kazin E. A., Blanton M. R., Scoccimarro R., McBride C. K., Berlind A. A., 2009, ApJ, 719, 1032
Kazin E. A., Sanchez A. G., Blanton M. R., 2011, MNRAS, submitted
Kessler R. et al., 2009, ApJS, 185, 32
Komatsu E. et al., 2011, ApJS, 192, 18
Lewis A., Challinor A., Lasenby A., 2000, ApJ, 538, 473
Marinoni C., Buzzi A., 2010, Nat, 468, 539
Martin D. et al., 2005, ApJ, 619, 1
Matsubara T., 2000, ApJ, 535, 1
Matsubara T., Suto Y., 1996, ApJ, 470, 1
Okumura T., Jing Y. P., 2011, ApJ, 726, 5
Outram P. J., Shanks T., Boyle B. J., Croom S. M., Hoyle F., Loaring N. S., Miller L., Smith R. J., 2004, MNRAS, 348, 745
Padmanabhan N., White M., 2008, Phys. Rev. D, 77, 3540
Percival W. J., White M., 2009, MNRAS, 393, 297
Percival W. J. et al., 2010, MNRAS, 401, 2148
Perlmutter S. et al., 1999, ApJ, 517, 565
Riess A. G. et al., 1998, AJ, 116, 1009
Riess A. G. et al., 1999, AJ, 117, 707
Riess A. G. et al., 2007, ApJ, 659, 98
Sahni V., Shafieloo A., Starobinsky A. A., 2008, Phys. Rev. D, 78, 3502
Samushia L. et al., 2011, MNRAS, 410, 1993
Seo H.-J., Eisenstein D. J., 2003, ApJ, 598, 720
Shafieloo A., 2007, MNRAS, 380, 1573
Shafieloo A., Clarkson C., 2010, Phys. Rev. D, 81, 3537
Shafieloo A., Alam U., Sahni V., Starobinsky A. A., 2006, MNRAS, 366, 1081
Shapiro C., Turner M. S., 2006, ApJ, 649, 563
Sharp R. et al., 2006, Proc. SPIE, 6269, 14
Simpson F., Peacock J. A., 2010, Phys. Rev. D, 81, 3512
Smith R. E. et al., 2003, MNRAS, 341, 1311
Sollerman J. et al., 2009, ApJ, 703, 2
Stern D., Jimenez R., Verde L., Kamionkowski M., Stanford A. S., 2010, J. Cosmol. Astropart. Phys., 2, 8
Taruya A., Nishimichi T., Saito S., 2010, Phys. Rev. D, 82, 3522
Taruya A., Saito S., Nishimichi T., 2011, Phys. Rev. D, 83, 3527
Wang Y., Tegmark M., 2005, Phys. Rev. D, 71, 3513
Wood-Vasey W. M. et al., 2007, ApJ, 666, 694
York D. G. et al., 2000, AJ, 120, 1579

This paper has been typeset from a TEX/LATEX file prepared by the author.